Scanning Tunneling Microscope (STM) was invented in the 80s by two physicists: G. Binnig and H. Rorher. They got the Nobel Prize a few years later. This invention paved the way for new possibilities in tunneling spectroscopy. Indeed, it provides a tool to measure the tunnel conductance at atomic scales. No other experimental setups are able to reach such precision.
The phenomenon behind STM is the quantum tunneling of electrons. When two electrodes are separated by a thin potential barrier such as an oxide or vacuum, electrons have a non-zero probability to tunnel through the barrier. This phenomenon, forbidden in classical physics is allowed in quantum mechanics. In scanning tunneling microscopy, the first electrode is the tip and the second one is the sample.
Before describing in more details the scanning tunneling microscope operating mode, the quantum phenomenon of tunneling will be developed.

## 3.1 Electron tunneling theory

The basic theory of tunneling has been introduced by the work of Bardeen [Bar61]. Because the particle wave function is not null in the barrier but decreases exponentially, the particle has a non-zero probability to tunnel through the barrier. The Bardeen model is useful to express the tunnel transmission of simple particles and quasiparticles. The two electrodes composing the tunnel junction are considered as independent systems in this approach. The tunnel current calculation as a function of the sample and tip density of states has been first developed for planar junctions. The measured current is thus averaged over the junction surface which is of the order of $\mathrm{mm}^2$ to $\mu\mathrm{m}^2$ for the smallest.
The particles transfer through the barrier is described by the Hamiltonian:

$$H = H_L + H_R + H_T \tag{3.1}$$

$H_L$ and $H_R$ are the Hamiltonians corresponding to the left and right electrodes. $H_T$ is the transfer Hamiltonian which is responsible for the transfer of electrons across the junction. Energy and eigenstates of $H_L$ et $H_R$ are respectively $E_\mu$, $\Psi_\mu$ and $E_\nu$, $\Psi_\nu$.
The tunneling current could be expressed as:

$$I = \frac{2\pi e}{\hbar} \sum_{\mu\ \nu} f(E_\mu)[1 - f(E_\nu + eV)]\ |M_{\mu\nu}|^2\ \delta(E_\mu - E_\nu) \tag{3.2}$$

With $f(E)$ the Fermi function and V the voltage drop across the junction. $M_{\mu\nu}$ is the matrix element of $H_T$ which couples eigenstates $\Psi_\mu$ of the tip and $\Psi_\nu$ of the surface.
Bardeen expressed this matrix element as follows:

$$M_{\mu\nu} = -\frac{\hbar^2}{2m} \int_{S_0} d\vec{S}[\Psi_\mu^* \vec{\nabla} \Psi_\nu - \Psi_\nu \vec{\nabla} \Psi_\mu^*] \tag{3.3}$$

With $S_0$ the surface of the two electrodes.

In order to understand tunneling in STM, the previous equation has to be reevaluated in terms of real space wave functions.
Tersoff and Hamann [TH83] performed the first calculation of the tunneling matrix element for the STM junctions. They took a simplified geometry for the electrodes.
Electrons of the tip in vacuum are described by an evanescent wave coming from the apex supposed to be a sphere of radius R and center $\mathrm{r}_0$:

$$\psi_\mu(r) = A_\mu \frac{e^{-\kappa|r - r_0|}}{|r - r_0|} \tag{3.4}$$

With

$$\kappa = \sqrt{2\mathrm{m}(\phi - \mathrm{E})/\hbar^2}$$

the inverse range of the evanescent wave of an electron which have an energy E in vacuum. $\phi$ is the work function. $\mathrm{A}_\nu$ is a renormalization constant.
To describe electronic states at the vicinity of the surface, Tersoff et Hamann considered a periodic crystal. The wave function $\psi_\nu$ of the sample in a given point $r$ of the tunnel barrier is thus a Bloch wave in the (xy) plane. This Bloch wave is weighted by an exponentially decreasing component along z:

$$\psi_\nu(r) = \psi_{k_{\shortparallel},E} = \sum_G C_{k_{\shortparallel},G}\ e^{i(k_{\shortparallel}+G)x}\ e^{-\alpha_{\nu,G}.z} \tag{3.5}$$

With $\alpha_{\nu,\mathrm{G}} = \sqrt{|\mathrm{k}_{\shortparallel} + \mathrm{G}|^2 + \mathrm{K}_\nu^2}$ and $\mathrm{K}_\nu = \sqrt{2\mathrm{m}(\phi - \mathrm{E})/\hbar^2}$. Here, $\mathrm{k}_{\shortparallel}$ is the wave vector component parallel to the surface. G is a wave vector of the reciprocal 2D lattice. $\mathrm{C}_{\mathrm{k}_{\shortparallel},\mathrm{G}}$ are the coefficients of the Fourier series development. Moreover, by supposing that tunneling voltages are small with respect to the workfunction and states are close to the Fermi surface, we obtain:

$$K_\mu = K_\nu = \frac{\sqrt{2m\phi}}{\hbar} \tag{3.6}$$

It assumes for simplicity that the work function is the same for the tip and the sample $\phi_\mu = \phi_\nu$.
By replacing (3.4) and (3.5) in (3.3):

$$M_{\mu\nu} = -\frac{2\pi\hbar^2}{m}\ A_\mu\ \psi_\nu(r_0) \tag{3.7}$$

Thus tunneling current can be written as:

$$I = \frac{(2\pi\hbar)^3}{m} \sum_{\nu\mu} A_\mu^2\ |\psi_\nu(r_0)|^2\ (f(E_\nu) - f(E_\mu))\ \delta(E_\nu - E_\mu + eV) \tag{3.8}$$

We supposed $\mathrm{A}_\mu$ to be constant, and by expressing the density of states in terms of wave functions, it comes:

$$I \propto \int dE\ \rho_s(r_0, E)\ \rho_p(E - eV)\ (f(E - eV) - f(E)) \tag{3.9}$$

Where $\rho_\mathrm{s}(\mathrm{r}_0, \mathrm{E}) = \sum_\nu |\psi_\nu(\mathrm{r}_0)|^2\ \delta(\mathrm{E} - \mathrm{E}_\nu)$ is the local density of states of the sample at the position of the tip apex which could be calculated from the formula (3.5).
The tunnel current expression can be generalized to:

$$I = \frac{e}{\hbar} \int_{-\infty}^{+\infty} dE\ \rho_s(r_0, E)\ \rho_p(E - eV)\ T(E, V, z)\ (f(E - eV) - f(E)) \tag{3.10}$$

With T(E,V,z) being the transmission factor of the tunnel barrier. This term contains the exponential dependence. As it is a function of z, it shows the deformation of the barrier for high voltage applied to the junction $\mathrm{V} \sim \phi/\mathrm{e}$. In STM, the voltage is always weak (less than typically 0.1V) compared to the tunnel barrier height $\phi$ and the Fermi energy $\mathrm{E_F}$. Thus, in our experiments, we could do the following approximation: $\mathrm{T(E, V, z)} \approx \mathrm{T(E_F, z)}$. Then:

$$I = \frac{eT(E_F, z)}{\hbar} \int_{-\infty}^{+\infty} dE\ \rho_s(r_0, E)\ \rho_p(E - eV)\ (f(E - eV) - f(E)) \tag{3.11}$$

Depending on the sign of the voltage, the tunneling current probes empty states (V>0) or filled states (V<0). The first experimental verification of the tunneling effect has been done by Giaver [Gia60] in the planar junction formed by a normal metal and a superconductor isolated by a thin oxide layer.

## 3.2 Tunneling spectroscopy of a superconductor

In the case of superconductors, when T<Tc, electrons couple in Cooper pairs which form a quantum condensate. This condensate is coherent on a macroscopic scale and is described by a global wavefunction. Condensation of Cooper pairs gives rise to a gap $\Delta$ in the excitation spectra. The conventional superconductors are described by the BCS theory in which the density of excitations is given by:

$$N_s(E) = N_s(0)\frac{E}{\sqrt{E^2-\Delta^2}} \quad for \quad |(E)| > \Delta, \quad or \quad 0 \quad otherwise. \tag{3.12}$$

Thus, tunneling spectroscopy gives information about the spatial and energetic repartition of the electronic excitations. At T=0K, there are no elementary excitations (quasiparticles) with energies below $\Delta$. It means that the current is zero when the voltage between the tip and the sample is lower than the gap divided by $e$ but is not null for higher voltages. The tunnel junction between a normal metal tip and a superconducting sample is depicted on figure 3.1.

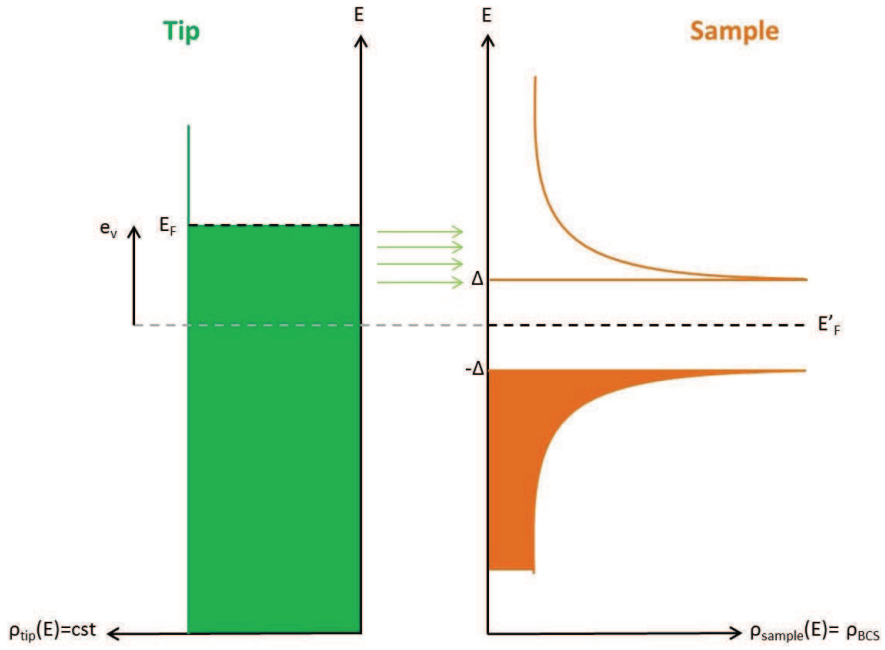


Figure 3.1: *Tunneling spectroscopy with a normal metal tip on a superconducting sample. On the left is the density of state of the tip (green) as a function of energy. On the right is the density of state of the sample (orange) as a function of energy. The occupied states are represented in plain color.*

## 3.3 Experimental aspects of STM

From the expression above, it is seen that the tunneling current $I_T$ exponentially depends on the tip-sample distance d. It is a key point to obtain a vertical resolution, on the z axis of the tip, of about a picometer:

$$I_T \sim e^{-2\kappa d} \tag{3.13}$$

With

$$\kappa = \sqrt{\frac{2m\Phi}{\hbar^2}}$$

In metals, the work function $\Phi$ is typically of 4eV. Thus, the tunnel current decreases by a factor 3 when increasing the tip-sample distance of 1Å.
The lateral resolution essentially depends on the wave functions and the tip-sample distance. Thus, STM provides an opportunity to obtain images in real space at atomic scale.
The tunneling regime is defined by three independents parameters:

- Distance between the two electrodes d (typically 5 to 10Å).
- Tunneling current $I_T$ ((typically 10-1000nA)).
- Tunneling bias $V_T$ (corresponding to the spectral window of interest, typically 0-100mV).

For stability reason and not to heat the sample, $I_T$ and $V_T$ are chosen in order to have tunnel resistance $R_T = V_T/I_T$ of 10MΩ to 1GΩ.

### 3.3.1 Topographic mode

The scanning tunneling microscope enables to collect topographic and spectroscopic data locally. There are two modes to reveal the topography of a surface (see figure 3.2).

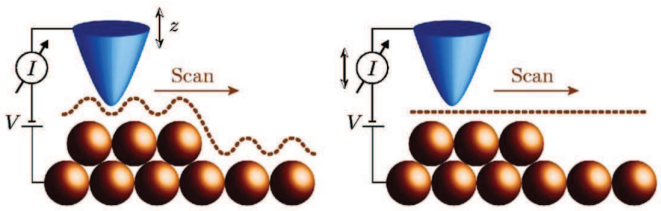


Figure 3.2: *Topographic STM modes. On the left: constant current imaging, distance z is adjusted to maintain the current constant. On the right: constant height imaging, the current I is changing.*

#### Constant current imaging

The constant current mode is the most often used in STM. Tunneling current is maintained constant by adjusting the vertical position of the tip during the scan. A feedback loop is used to control the distance d.
If the density of states is known as homogeneous on the studied area, then the profile corresponds to a constant tip-sample distance.
The vertical tip position z is recorded as a function of lateral coordinates (x,y). It is encoded in color or grey scale to form artificial maps called "topographic image".
The scan speed is limited by the bandwidth of the feedback loop which is typically of the order of the kiloHertz.

**Constant height imaging**

When using this imaging mode, the tip which scans the sample is maintained at a constant height. Thus, the feedback loop is open. Variations in the tunneling current are due to variations of the sample density of states.
Fluctuations of the current as a function of the tip position represents the surface topography, provided spatially constant state density.
This imaging mode permits to increase the scan speed, since it does not require the feedback loop to function. However, its utilisation is limited to surfaces with a roughness less than few Angströms, namely the tip-surface distance. Indeed, high protrusions could generate collisions between the tip and the sample surface.

### 3.3.2 Spectroscopic mode

By varying the bias voltage while maintaining the tip fixed above a given sample location, one can have a direct access to the electronic density of states.
When applying a positive voltage on the sample, electrons tunnels to allowed empty states of the sample. Conversely, when applying a negative voltage, electrons tunnels from occupied states of the sample. It can be seen on the figure 3.1.
dI/dV(V) spectra can be obtained from a numerical derivative of acquired I(V) curves or by using a lock-in amplification technique. In both cases, tunnel conductance is a local measure of the sample density of states. Measuring it in each point of the surface permits to construct a conductance map spatially associated to the topographic map.
In the experimental setup M3, the lowest temperature available is 300mK. However, the duration of one temperature cycle last less than 40h. It is thus essential to determine the duration of the acquisition before starting the measurements. In table 3.1 are the typical parameters of the measurements that were used to acquire the conductance maps and the topography on the experimental setup M3. The topographic measurements last about one hour and the spectroscopic measurements last about 19 hours. Thus, the total acquisition time for the topography/spectroscopy data simultaneously is 20 hours.

The scanning tunneling microscopy is a very sensitive tool and mechanical noises can perturb the measurements. The electronics system can also add some noise during the acquisition of the data. An automatic filtering can be used to remove these noises effects. During this thesis, the amplitude of the noise has been reduced by using a Gaussian filtering. Then, a Median filtering has been applied to the conductance maps to remove the spectra that were completely saturated. This filter compares the neighbouring values and changes it only if there is a big difference. It corresponds to only few spectra in the conductance map.

| **Topographic parameters** | |
|---|---|
| Scan size | 300nm x 300nm |
| Pixel | 512 x 512 |
| Scan speed | 30nm/s |
| It | 150pA |
| Vt | 500mV |
| **Spectroscopic parameters** | |
| Grid size | 256 x 256 |
| Points/spectra | 512 |
| Energy range | [-6mV;+6mV] |
| Acquisition time | 2ms/pts |
| Is | 250pA |
| Vs | -50mV |

Table 3.1: *Typical example of the measurement procedure that was used to acquire the conductance map and its corresponding topography. The total acquisition time for the topography and spectroscopy data simultaneously last about 20 hours.*

### 3.3.3 Piezoelectric effect

In scanning tunneling microscope, piezoelectric compounds are needed to realize very short displacements of the tip in the three space directions and thus visualize the atoms on a surface. The piezoelectric effect is the property of certain crystals to generate charges when stressed. This effect is due to the intrinsic polarization of the crystalline unit cell, and more generally to a non-centro-symmetric charge distribution (see figure 3.3).
When a crystalline cell with a non uniform charge distribution is mechanically deformed, the geometric centers of positive and negative charges move by a different amount resulting in an electric polarization. Conversely, the application of an electrical field results in different motions of the charges geometric centers in the cell, that finally induces a macroscopic deformation of the material, either shear or longitudinal.
In the STM, piezoelectric tubes with three electrodes are used (see figure 3.3). The first electrode is used for the vertical displacements along the z axis. The two others pairs of electrodes are used for the scanning movement in the (x,y) plane.

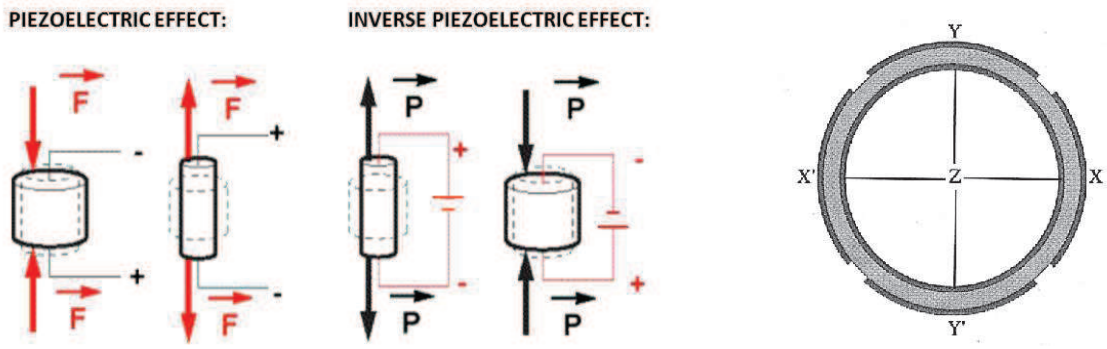


Figure 3.3: *Left: Schematic view of the piezoelectric effect. When applying a mechanical stress to the tube, it generates an electric polarization. When applying an electrical field, namely a voltage to the tube, a macroscopic deformation is induced. Right: Piezoelectric tube with 3 electrodes (x,y,z) (top view).*

### 3.3.4 Vibration isolations

Atomic resolution and stable spectroscopy can be obtained only if the system is well isolated from external mechanical vibrations. For all microscopes used during this thesis, two solutions were implemented.
First, STM heads are made as small and as light as possible, in order to increase their mechanical resonant frequency. The heads are isolated from the environment by a spring-mass low-pass filters. In our cases 3 STMs used in this work were made of Titanium and ceramics.
The second isolation stage consist of pneumatic anti-vibrational dampers, alimented by compressed air. The dampers (3 or 4) support all the system including the STM, chambers, pumps and a part of electronics. It enables to effectively isolate the microscope from environment mechanical perturbations.